Ann Nucl Med (2018) 32:1–6
DOI 10.1007/s12149-017-1215-y

ORIGINAL ARTICLE

# Influence of region-of-interest determination on measurement of signal-to-noise ratio in liver on PET images

**Shinji Amakusa[1] · Koki Matsuoka[1] · Masayuki Kawano[1] · Kiyotaka Hasegawa[1] · Mio Ouchida[1] · Ayaka Date[1] · Tsuyoshi Yoshida[2] · Masayuki Sasaki[3]**

Received: 30 June 2017 / Accepted: 22 September 2017 / Published online: 20 October 2017


**Abstract**
*Objective* On $^{18}$F-fluoro-2-deoxy-D-glucose ($^{18}$F-FDG) positron emission tomography (PET), signal-to-noise ratio in the liver ($SNR_{liver}$) is used as a metric to assess image quality. However, some regions-of-interest (ROIs) are used when measuring the $SNR_{liver}$. The purpose of this study is to examine the different ROIs and volumes of interest (VOIs) to obtain a reproducible $SNR_{liver}$.
*Methods* This study included 108 patients who underwent $^{18}$F-FDG-PET/CT scans for the purpose of cancer screening. We examined four different ROIs and VOIs; a 3-cm-diameter and a 4-cm-diameter circular ROI and a 3-cm-diameter and a 4-cm-diameter spherical VOI on the right lobe of the patients' livers. The average of SUV ($SUV_{mean}$), standard deviation (SD) of SUV ($SUV_{SD}$), $SNR_{liver}$ and SD of the $SNR_{liver}$ obtained using ROIs and VOIs were then compared.
*Results* Although the $SUV_{mean}$ was not different among the ROIs and VOIs, the $SUV_{SD}$ was small with a 3-cm-diameter ROI. The largest $SUV_{SD}$ was obtained with a 4-cm-diameter spherical VOI. The $SNR_{liver}$ and the SD of the $SNR_{liver}$ with a 4-cm-diameter spherical VOI were the smallest, while those with a 3-cm-diameter circular ROI were the largest. These results suggest that a small ROI may be placed on a relatively homogeneous region not representing whole liver unintentionally.
*Conclusion* The $SNR_{liver}$ varied according to the shape and size of ROIs or VOIs. A 4-cm-diameter spherical VOI is recommended to obtain stable and reproducible $SNR_{liver}$.

**Keywords** FDG-PET · Quality control · Image quality · Signal-to-noise ratio in the liver · Region of interest

✉ Masayuki Sasaki
msasaki@hs.med.kyushu-u.ac.jp

[1] Department of Radiological Technology, Koga Hospital 21, Kurume, Japan

[2] PET Imaging and Diagnostic Center, Koga Hospital 21, Kurume, Japan

[3] Department of Health Sciences, Graduate School of Medical Sciences, Kyushu University, Fukuoka, Japan

## Introduction

$^{18}$F-fluoro-2-deoxy-D-glucose ($^{18}$F-FDG) positron emission tomography (PET) has been widely used for detecting malignant tumors, differential diagnosis, determination of therapeutic strategy, monitoring treatment response and also in follow-up examinations [1–10]. Standardized uptake value (SUV) is a parameter used to evaluate $^{18}$F-FDG accumulation semiquantitatively. In addition, quantitative accuracy and reproducibility of SUV are especially important for differential diagnosis and for monitoring treatment response. Therefore, routine inspection and quality assessment of PET scanners are necessary to maintain accurate quantification during the PET examinations [11, 12]. Noise equivalent count (NEC) has been used as a standard metric to assess the performance of a PET scanner [13–16]. NEC describes the equivalent coincidence counts that would have the same noise properties as the net true counts, corrected for random and scattered coincidences. NEC reflects the quality of acquired raw data, and thus does not take into account the impact of reconstruction algorithms or correction methods. Recently, the incorporation of additional information, such as point-spread function and time-of-flight information, into iterative reconstruction algorithm markedly improved the quality of the PET image [17]. Signal-to-noise ratio in the liver ($SNR_{liver}$) is used as a metric to evaluate image quality

obtained from reconstructed images. $SNR_{liver}$ has been reported to be useful for determining the injection dose of $^{18}$F-FDG in relation to the patient's body weight and the optimization of the acquisition time [18–22].

However, a poor correlation has also been reported between $SNR_{liver}$ and the result of the visual evaluation of clinical images [14, 15]. Because the $^{18}$F-FDG uptake in the liver is not homogeneous, the placement of the regions-of-interest (ROIs) for the liver was considered to affect the stability and reproducibility of the $SNR_{liver}$ [23]. Although the guidelines for the oncology $^{18}$F-FDG-PET/CT data acquisition protocol recommended placing a circular ROI with 3 cm diameter in the right lobe of the liver in a coronal image, various other methods have been also reported [17–22, 24, 25]. Furthermore, a spherical volume-of-interest (VOI) with 3 cm diameter for measurement the SUV of the liver has also been reported to be highly reproducible [26]. Therefore, the most appropriate method for placing an ROI, which provides a stable and reproducible $SNR_{liver}$ needs to be established.

The aim of this study is to compare the effects of different ROIs and VOIs on measurement of $SNR_{liver}$s, and to determine the most reproducible method to measure $SNR_{liver}$.

## Materials and methods

### Subjects

This retrospective study was approved by the institutional review board of our hospital, and a written informed consent was waived. This study included 108 patients (67 men and 41 women, mean age $57.2 \pm 11.0$ years, mean body weight $65.1 \pm 12.9$ kg, mean body mass index (BMI) $23.7 \pm 3.2$ kg/m$^2$) who underwent $^{18}$F-FDG-PET/CT scan for the purpose of cancer screening. Patients with abnormal accumulations in the liver, those with a high blood-sugar level more than 110 mg/dL, those with liver dysfunction and those with a liver too small to place ROIs were excluded from this study.

### Scanner description

PET/CT data were acquired using a True Point Biograph 40 scanner (Siemens AG, Munich, Germany). This scanner is comprised of 39 rings, with a total of 144 lutetium oxyorthosilicate (LSO) detectors, covering an axial field of view (FOV) of 16.2 cm and a transaxial FOV of 68.3 cm in diameter. Each LSO crystal is $4 \times 4 \times 20$ mm$^3$.

### $^{18}$F-FDG-PET/CT protocol

The patients fasted for approximately 6 h before $^{18}$F-FDG administration. The dose of $^{18}$F-FDG was 3.7 MBq/kg for patients weighing 70 kg or less and 259 MBq for patients heavier than 70 kg. After the administration of $^{18}$F-FDG, the patient rested in a dimmed room for an hour before the PET/CT scan was started. The patients were scanned with their arms down. Scan duration of one bed position was 2 min. The overlap ranges of PET data acquisition were 28%. The CT scan for attenuation correction was performed according to the following parameters: 120 kVp, 80 mAs, collimation $24 \times 1.2$ mm, pitch 0.8, 0.5 s per one rotation. The diameter of the FOV of CT images was 70 cm. The slice thickness of the reconstructed CT image was 5 mm with a 3 mm interval.

Scatter correction was performed using the single scatter simulation method. PET acquisition data were reconstructed using the method of Fourier rebinning two-dimensional ordered subset expectation maximization (FORE–OSEM) with two iterations and eight subsets, and were then smoothed with a Gaussian filter with a full width at half maximum (FWHM) of 6 mm. The slice thickness of PET images was 5 mm and the interval of slices was 3 mm.

### Data analysis

For data analysis, the VOXBASE II fusion viewer (J-mac system, Sapporo, Japan) was used. Circular ROIs with

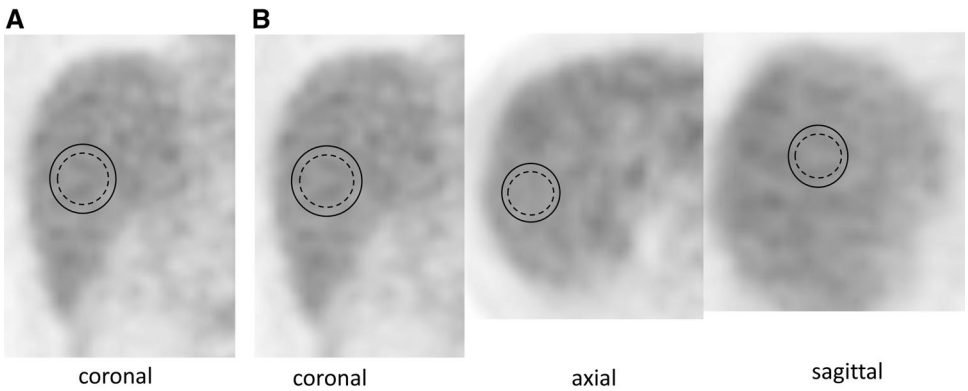


**Fig. 1** Placement of an ROI and a VOI. **a** Circular ROIs with a diameter of 3 cm (dashed line) and 4 cm (solid line) were placed on the right lobe of the liver on consecutive five coronal images. **b** Spherical VOIs with a diameter of 3 cm (dashed line) and 4 cm (solid line) were placed on the right lobe of the liver in three-dimensional volume data five times

a diameter of 3 cm ($ROI_3$; 6.72 $cm^2$) and of 4 cm ($ROI_4$; 13.43 $cm^2$) were placed on the right lobe of the liver on five consecutive coronal images ($i = 1$–5) (Fig. 1a). ROIs were carefully placed on the center of the right lobe of the liver, taking care not to include the hepatic portal region and subphrenic region. Spherical VOIs with a diameter of 3 cm ($VOI_3$; 13.82 $cm^3$) and of 4 cm ($VOI_4$; 32.83 $cm^3$) were placed on the right lobe of the liver in 3 dimensional volume data (Fig. 1b). The VOI placement was repeated five times ($j = 1$–5). The average and standard deviation of SUV within each ROI and VOI were calculated as $SUV_{mean}$ and $SUV_{SD}$, respectively.

The $SNR_{liver,i}$ with an ROI and the $SNR_{liver,j}$ with a VOI were defined with the following formulae.

$$SNR_{liver,i} = \frac{SUV_{mean,i}}{SUV_{SD,i}}, \text{ in the case of circular ROIs,}$$

$$SNR_{liver,j} = \frac{SUV_{mean,j}}{SUV_{SD,j}}, \text{ in the case of spherical VOIs,}$$

where $i$ and $j$ represent the number of an ROI or a VOI on each patient.

$SNR_{liver}$ was calculated by the following formulae using the values of five ROIs or VOIs.

$$SNR_{liver} = \frac{1}{5}\left(\sum_{i=1}^{5} SNR_{liver,i}\right), \text{ in the case of circular ROIs,}$$

$$SNR_{liver} = \frac{1}{5}\left(\sum_{j=1}^{5} SNR_{liver,j}\right), \text{ in the case of spherical VOIs,}$$

SD of the $SNR_{liver,i}$ and $SNR_{liver,j}$ was also calculated, respectively.

### Statistical analysis

Comparisons of the mean of $SUV_{mean}$, $SUV_{SD}$ and $SNR_{liver}$ among different ROIs and VOIs were performed by one-way ANOVA, followed by a post hoc Tukey HSD test. Comparison of the SD of $SNR_{liver,i}$ and $SNR_{liver,j}$ among ROIs and VOIs was performed in the same way for the purpose of determining the stability of measurement of $SNR_{liver}$ in each ROI. We used a level of significance of $p < 0.05$.

## Results

Figure 2 shows the comparison of the mean $SUV_{mean}$s among two ROIs and two VOIs. $SUV_{mean}$s were not significantly different among any ROIs or VOIs. On the other hand, Fig. 3 shows that the $SUV_{SD}$s with $ROI_3$ were significantly lower than those with others. $SUV_{SD}$ with $ROI_4$ was also significantly lower than that with $VOI_4$. $SUV_{SD}$s with VOIs were not significantly different from each other.

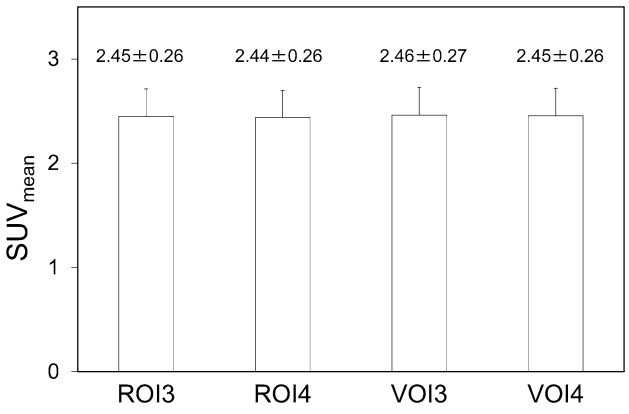


**Fig. 2** Comparison of $SUV_{mean}$ among ROIs and VOIs. $SUV_{mean}$s were not significantly different among any ROIs or VOIs ($p = 0.94$)

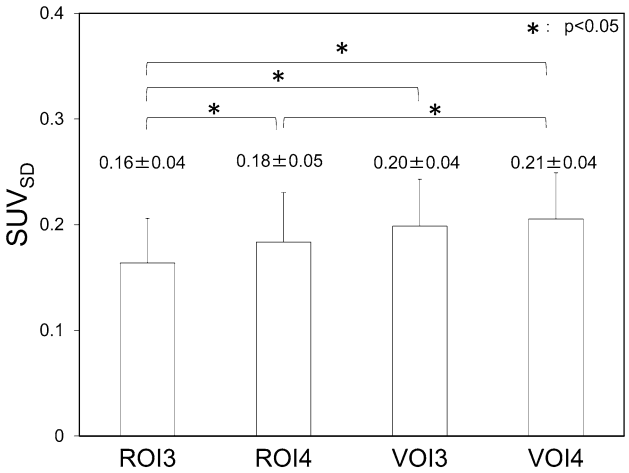


**Fig. 3** Comparison of $SUV_{SD}$ among ROIs and VOIs. The mean value of $SUV_{SD}$ with $ROI_3$ was significantly lower than those with others. $SUV_{SD}$ with $ROI_4$ was also significantly lower than that with $VOI_4$ but was not significantly lower than that with $VOI_3$ ($p = 0.06$). $SUV_{SD}$s with VOIs did not significantly differ from each other

Figure 4 shows the comparison of $SNR_{liver}$s among two ROIs and two VOIs. $SNR_{liver}$s with two ROIs and two VOIs were significantly different from each other, and $SNR_{liver}$s with $ROI_3$ was the highest, followed by $ROI_4$, $VOI_3$ and $VOI_4$.

Figure 5 shows the comparison of the SDs of $SNR_{liver,i}$ and $SNR_{liver,j}$ among two ROIs and two VOIs. The SD of $VOI_4$ was lower than those of $VOI_3$, $ROI_4$ and $ROI_3$ in ascending order. Each SD had a significant difference from the others.

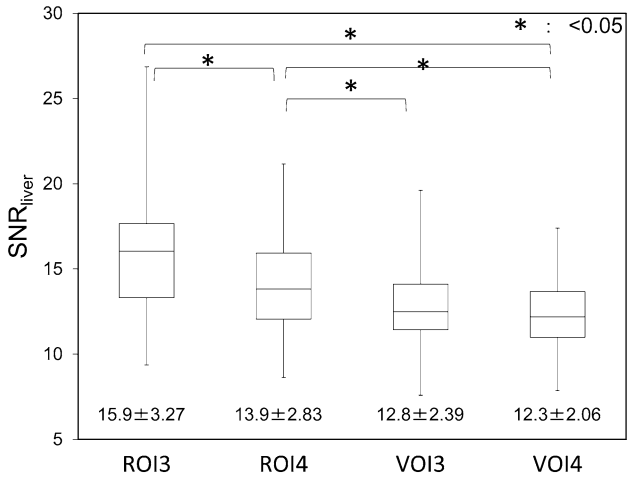


**Fig. 4** $SNR_{liver}$s of ROIs and VOIs. $SNR_{liver}$s with two ROIs and two VOIs were significantly different from each other. $SNR_{liver}$s with $ROI_3$ was the highest followed by $ROI_4$, $VOI_3$ and $VOI_4$

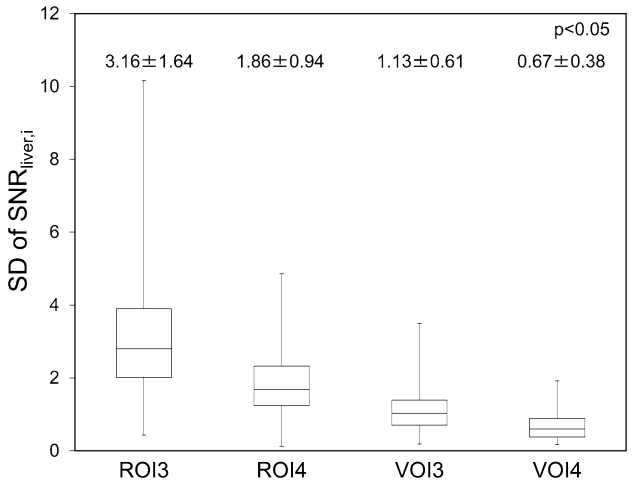


**Fig. 5** The standard deviations of $SNR_{liver}$ of ROIs and VOIs. The SD of $VOI_4$ was lower than those of $VOI_3$, $ROI_4$ and $ROI_3$ in ascending order. Each SD showed a significant difference from the others

## Discussions

In this study, we investigated the influence of ROI or VOI determination on the stability and reproducibility of $SNR_{liver}$ to evaluate PET image quality. Although the $SUV_{mean}$ was not different among ROIs and VOIs, the $SUV_{SD}$ was small with a small ROI. Furthermore, a small ROI resulted in a large $SNR_{liver}$ and large SD of $SNR_{liver}$.

The difference in $SUV_{mean}$s among ROIs and VOIs were not statistically significant. This suggests that a similar $SUV_{mean}$ of the liver can be obtained when using either the diameter of 3 or 4 cm circular ROIs or spherical VOIs. On the other hand, the $SUV_{SD}$ with $ROI_3$ was smaller than those with other ROI and VOIs. This is presumably dependent on the region where the ROI is placed. Manual placement of a small ROI tended to be restricted to homogeneous regions unintentionally. Thus, it may not represent the general variability of the liver SUV. Therefore, the placement of a relatively large ROI is recommended to represent the general FDG uptake and distribution in the liver. $SNR_{liver}$ with $ROI_3$ was the largest, and was followed by those with $ROI_4$, $VOI_3$ and $VOI_4$ in descending order. As the $SUV_{mean}$ was not significantly different among all ROIs and VOIs, the difference of $SNR_{liver}$ among ROIs and VOIs was considered to result from the difference in $SUV_{SD}$. In our study, the SD of $SNR_{liver}$ with $ROI_3$ was also the largest and was followed by those with $ROI_4$, $VOI_3$ and $VOI_4$. Thus, the $SNR_{liver}$ with $VOI_4$ is considered to be the most reproducible among the ROIs and VOIs. McDermott et al. used a spherical VOI with a diameter of 5 cm and showed a small SD of $SNR_{liver}$ [25]. From the findings described above, we have concluded that the measurement of $SNR_{liver}$ with a smaller ROI is not reproducible, and that to obtain a reproducible $SNR_{liver}$, it is necessary to place a sufficiently large VOI.

Concerning the manual placement of an ROI or a VOI, placing a circular ROI has a higher degree of freedom than a spherical VOI. Therefore, the variation of measured values should become larger with circular ROIs. Some methods such as increasing the number of measurements is recommended when using a circular ROI [17]. With a larger diameter of ROI or VOI, the degree of freedom when placing an ROI was low, and then the deviation of measurement of $SUV_{SD}$ became smaller. However, placing ROI or VOI with too large of a diameter may be difficult in some cases in which the patient has a small liver.

In this study, a single researcher performed data analysis. Thus, the variance indicates the intra-observer difference for ROI analysis. Our results showed that the SD of $SNR_{liver}$, which was an intra-observer variance, was small in both large ROIs and large VOIs. Viner et al. examined the inter-observer agreement of $SUV_{mean}$ normalized with lean body mass in the liver [26]. They used a VOI with a 3 cm diameter and showed a good inter-observer agreement of $SUV_{mean}$ measurements. An inter-observer variance is generally considered to be larger than an intra-observer variance [27, 28]. This suggests that using a larger VOI with a 4 cm diameter can be expected to obtain better results. Although we did not examine the inter-observer variance of $SNR_{liver}$ at this time, we predict it would be larger but have a similar tendency to the intra-observer variance of $SNR_{liver}$. Further examination is required to elucidate the effect of ROIs and VOIs on the inter-observer variance of $SNR_{liver}$.

$SNR_{liver}$ itself is considered to be unstable as an index of the image quality. Primarily, the administered dose of $^{18}$F-FDG is a potential influencing factor in the reliability of SUV [29]. A relatively low administered dose generally

results in impaired image quality due to low count statics. This effect also influences the SNR measurement. We suppose that the SD of SNR measured with a small ROI may be larger than with a larger ROI due to variance of SUV resulting from increasing image noise in the liver. Therefore, we infer that reproducibility of SNR measurement would also be improved with a large ROI in the case of a low administered dose. In addition, as the administered dose in this study was determined based on the patient body weight, the influence of the administered dose on the results should be considered negligible, with the exception of possible calibration errors by the dose calibrator. On the other hand, at institutions where $^{18}$F-FDG is supplied by venders, the administered dose cannot easily be adjusted, which may affect the reliability of SUV, as a result of SNR. Secondly, patients with a large BMI are reported to show high normal organ SUVs due to copious adipose tissue, which does not accumulate $^{18}$F-FDG [30–32]. A lean body mass is recommended when calculating regular tissue SUV due to potentially increased values in patients with a high BMI [30–32]. Moreover, in the case of an obese patient, image quality is deteriorated by increases in the number of random and scattered coincidences, and thus patient body weight influences the SNR measurement. However, the effect of body weight as a normalization factor for calculating SUV is negligible in SNR derived as the ratio of $SUV_{mean}$ to $SUV_{SD}$. In addition, patient body weight was not considered to be a variable in this study, as no patient was of a weight that could be deemed as having an effect on regular tissue SUV. Third, underestimation of liver SUV near the diaphragm due to respiratory movement sometimes occurs in cases involving a small liver. The SUV in the dorsal region of the right lobe of the liver is frequently low, due to an artifact associated with arm motion. The ROIs or VOIs must be carefully placed to avoid such regions. Fourth, this study did not include patients with liver dysfunction, because the liver FDG uptake in patients with liver dysfunction has been reported to be decreased and heterogeneous, and so the $SNR_{liver}$ of such patients needs to be analyzed in separate investigations [23, 33].

## Conclusion

To obtain a stable and reproducible $SNR_{liver}$, a 4-cm-diameter spherical VOI is considered as superior to a 3-cm-diameter spherical VOI, a 3-cm-diameter and 4-cm-diameter circular ROI.

**Compliance with ethical standards**

**Conflict of interest** No potential conflicts of interest were disclosed

## References


1. Lindell RM, Hartman TE, Swensen SJ, Jett JR, Midthun DE, Nathan MA, et al. Lung cancer screening experience: a retrospective review of PET in 22 non-small cell lung carcinomas detected on screening chest CT in a high-risk population. Am J Roentgenol. 2005;185:126–31.
2. Cronin P, Dwamena BA, Kelly AM, Carlos RC. Solitary pulmonary nodules: meta-analytic comparison of cross-sectional imaging modalities for diagnosis of malignancy. Radiology. 2008;246:772–82.
3. Nomori H, Watanabe K, Ohtsuka T, Naruke T, Suemasu K, Uno K. The size of metastatic foci and lymph nodes yielding false-negative and false–positive lymph node staging with positron emission tomography in patients with lung cancer. J Thorac Cardiovasc Surg. 2004;127:1087–92.
4. Lee JH, Rosen EL, Mankoff DA. The role of radiotracer imaging in the diagnosis and management of patients with breast cancer: part 1—overview, detection, and staging. J Nucl Med. 2009;50:569–81.
5. Lee JH, Rosen EL, Mankoff DA. The role of radiotracer imaging in the diagnosis and management of patients with breast cancer: part 2—response to therapy, other indications, and future directions. J Nucl Med. 2009;50:738–48.
6. Kato H, Miyazaki T, Nakajima M, Takita J, Kimura H, Faried A, et al. The incremental effect of positron emission tomography on diagnostic accuracy in the initial staging of esophageal carcinoma. Cancer. 2005;103:148–56.
7. van Vliet EPM, Heijenbrok-Kal MH, Hunink MGM, Kulpers EJ, Siersema PD. Staging investigations for oesophageal cancer: a meta analysis. Br J Cancer. 2008;98:547–57.
8. Israel O, Yefremov N, Bar-Shalom R, Kagana O, Frenkel A, Keidar Z, et al. PET/CT detection of unexpected gastrointestinal foci of $^{18}$F-FDG uptake: incidence, localization patterns, and clinical significance. J Nucl Med. 2005;46:758–62.
9. Bares R, Klever P, Hauptmann S, Hellwig D, Fass J, Cremerius U, et al. F-18 fluorodeoxyglucose PET in vivo evaluation of pancreatic glucose metabolism for detection of pancreatic cancer. Radiology. 1994;192:79–86.
10. Bang S, Chung HW, Park SW, Chung JB, Yun M, Lee JD, et al. The clinical usefulness of 18-fluorodeoxyglucose positron emission tomography in the differential diagnosis, staging, and response evaluation after concurrent chemoradiotherapy for pancreatic cancer. J Clin Gastroenterol. 2006;40:923–9.
11. Belakhlef S, Church C, Hays A, Fraser R, Lakhanpal S. Quantitative assessment of the influence of location, internal temperature, idle time, and normalization on the sensitivity of a mobile PET/CT scanner. J Nucl Med Technol. 2008;36:147–50.
12. Watanuki S, Tashiro M, Miyake M, Ishikawa Y, Itoh M, Yanai K, et al. Long-term performance evaluation of positron emission tomography: analysis and proposal of a maintenance protocol for long-term utilization. Ann Nucl Med. 2010;24:461–8.
13. de Kemp R, Caldwell C, Farncombe T, McKee B, Wassenaar R, Wells R, et al. PET imaging standards and quality assurance for the multi-center trials of the Ontario Clinical Oncology Group. J Nucl Med. 2006;47:365P.
14. Mizuta T, Senda M, Okamura T, Kitamura K, Inaoka Y, Takahashi M, et al. NEC density and liver ROI S/N ratio for image quality control of whole-body FDG-PET scans: comparison with visual assessment. Mol Imaging Biol. 2009;11:480–6.
15. Fukukita H, Senda M, Terauchi T, Suzuki K, Daisaki H, Matsumoto K, et al. Japanese guideline for the oncology FDG-PET/CT data acquisition protocol: synopsis of version 1.0. Ann Nucl Med. 2010;24:325–34.

16. Strother SC, Casey ME, Hoffman EJ. Measuring PET scanner sensitivity: relating countrates to image signal-to-noise ratio using noise equivalent counts. IEEE Trans Nucl Sci. 1990;37:783–8.
17. Akamatsu G, Ishikawa K, Mitsumoto K, Taniguchi T, Ohya N, Baba S, et al. Improvement in PET/CT image quality with a combination of point-spread function and time-of-flight in relation to reconstruction parameters. J Nucl Med. 2012;53:1716–22.
18. Masuda Y, Kondo C, Matsuo Y, Uetani M, Kusakabe K. Comparison of imaging protocols for $^{18}$F-FDG PET/CT in overweight patients: optimizing scan duration versus administered dose. J Nucl Med. 2009;50:844–8.
19. Nagaki A, Onoguchi M, Matsumoto N. Patient weight-based acquisition protocols to optimize $^{18}$F-FDG PET/CT image quality. J Nucl Med Technol. 2011;39:72–6.
20. de Groot EH, Post N, Boellaard R, Wagenaar NR, Willemsen ATM, van Dalen JA. Optimized dose regimen for whole-body FDG-PET imaging. EJNMMI Res. 2013;3:63.
21. Geismar JH, Stolzmann P, Sah BR, Burger IA, Seifert B, Delso G, et al. Intra-individual comparison of PET/CT with different body weight-adapted FDG dosage regimens. Acta Radiol Open. 2015;4:1–9.
22. Yan J, Schaefferkoetter J, Conti M, Townsend D. A method to assess image quality for low-dose PET: analysis of SNR, CNR, bias and image noise. Cancer Imaging. 2016;16:26.
23. Irie S, Hayashida N, Shinkawa T, Kamasaki T, Matsunaga A, Miyamoto I, et al. Clinical usefulness of $^{18}$F-FDG PET/CT for the screening of metabolic liver disorders. Life Sci J. 2014;11:99–104.
24. Chang T, Chang G, Clark JW, Diab RH, Rohren E, Mawlawi OR. Reliability of predicting image signal-to-noise ratio using noise equivalent count rate in PET imaging. Med Phys. 2012;39:5891–900.
25. McDermott GM, Chowdhury FU, Scarsbrook AF. Evaluation of noise equivalent count parameters as indicators of adult whole-body FDG-PET image quality. Ann Nucl Med. 2013;27:855–61.
26. Viner M, Mercier G, Hao F, Malladi A, Subramaniam RM. Liver $SUL_{mean}$ at FDG PET/CT: interreader agreement and impact of placement of volume of interest. Radiology. 2013;267:596–601.
27. Rudd JHF, Myers KS, Bansilal S, Machac J, Pinto CA, Tong C, et al. Atherosclerosis inflammation imaging with $^{18}$F-FDG PET: carotid, iliac, and femoral uptake reproducibility, quantification methods, and recommendations. J Nucl Med. 2008;49:871–8.
28. Goh V, Shastry M, Engledow A, Kozarski R, Peck J, Endozo R, et al. Integrated $^{18}$F-FDG PET/CT and perfusion CT of primary colorectal cancer: effect of inter- and intraobserver agreement on metabolic-vascular parameters. AJR. 2012;199:1003–9.
29. Chang DW, Ersahin D, Staib LH, Della Latta D, Giorgetti A, d'Errico F. Using SUV as a guide to $^{18}$F-FDG dose reduction. J Nucl Med. 2014;55:1–5.
30. Boellaard R. Standards for PET image acquisition and quantitative data analysis. J Nucl Med. 2009;50:11S-20S.
31. Adams MC, Turkington TG, Wilson JM, Wong TZ. A systematic review of the factors affecting accuracy of SUV measurements. AJR. 2010;195:310–20.
32. Wahl RL, Jacene H, Kasamon Y, Lodge MA. From RECIST to PERCIST: evolving considerations for PET response criteria in solid tumors. J Nucl Med. 2009;50:122S-150S.
33. Abikhzer G, Alabed YZ, Azoulay L, Assayag J, Rush C. Altered hepatic metabolic activity in patients with hepatic steatosis on FDG PET/CT. AJR 2011;196:176–80.